Research Article

Experiment on Corrosion Fatigue Life of Steel Strands under the Coupling Effects of Chloride Environment and Alternating Loads

Guowen Yao [1,2] **Xuanrui Yu,** [1] **Lifeng Gu,** [1] **and Yixing Jiang** [1]

[1]*Chongqing JiaoTong University, Chongqing 400074, China*
[2]*State Key Laboratory of Mountain Bridge and Tunnel Engineering, Chongqing 400074, China*

Correspondence should be addressed to Xuanrui Yu; 611190080010@mails.cqjtu.edu.cn

Corrosion pits will lead to local stress concentration on the surface of steel strands and even shorter fatigue life and worse mechanical properties of steel strands. In order to explore the corrosion mechanics of steel strands to predict the fatigue life, accelerated salt spray corrosion test is carried out to simulate the corrosion laws of steel strands and record the changes of the corrosion degrees during the experiment, considering the coupling effects of alternating loads and chloride environment. Besides, the impact of stress amplitudes on the corrosion degrees of steel strands is quantitatively studied by the corrosion weight loss, and corroded steel strands in experiment are graded according to the corrosion weight loss to test the mechanical properties, respectively; the results show that the corrosion weight loss and tensile strength of steel strands obey the exponential distribution, and the relationship with elongation is linear. In addition, the relationships between the stress concentration coefficient and the pit length, width, and depth are obtained; with the three-dimensional linear regression theory, the accuracy of the regression model is verified by t-value test, laying a foundation for predicting the corrosion life of the cables.

1. Introduction

Steel strands have been widely used in stayed bridge and suspension bridge. Chloride-induced corrosion of steel structure is one of the main factors for the durability of steel strands exposed to the salt fog environment; this can cause the corrosion of steel strands and ultimately shorten the durability and serviceability of stayed bridge [1]. Therefore, it is necessary to build a predicted model to investigate the fatigue life of the steel strands with pits in different size.

The steel strands consist of multisteel wires with a high strength often used in cables. This structure will usually lose effectiveness under the variable road and the salt fog environment. However, most of the literatures mainly consider the effects caused by the variable stress to the fatigue life of steel strands. Suzumura and Nakamura [1] investigated the stress intensity factor (SIF) for long cracks to predict the fatigue life of steel strands by theoretical analysis, under the variable load. The result shows that the defect size that should be used to calculate the SIF is larger than the

inclusion size itself. It means that the prediction fatigue life of steel strands is not standard always lower than that in actual condition. Verpoest et al. [2, 3] analysed the fatigue life of steel strands affected by the fatigue threshold, surface condition, and fatigue limit based on the fracture mechanics. It was found that the fatigue threshold is a main factor to influence the fatigue life of steel strands. A model was established by Lambrighs et al. [4] to quantify the fatigue life of steel strands, and the results indicate that the fatigue threshold is about 3 MPa–5 MPa, when the stress over this regions will result in the expansion of crack.

From the abovementioned analysis, these literatures only consider the fatigue life of steel strands affected by the variable stress, but for the chloride-induced corrosion to the steel strand was not considered. In chloride salt environment, the electrochemical reaction among steel strands, water, and chloride ion is easy to take place, where chloride ions play the role of catalyst. Consequently, once the reaction occurs, it will continue until the strand breaks [5]. The corrosion types are mainly divided into hydrogen absorption

corrosion and oxygen absorption corrosion. Hydrogen absorption corrosion is easy to happen in acid environment, while oxygen absorption corrosion occurs more common in alkaline or neutral environment, and corrosion pits will appear gradually on the surface of steel strands during corrosion process, leading to local stress concentration phenomenon around pits, which is fatal for the fatigue life of cables. The conclusion was drawn by Valor et al. [6]. Besides, local stress is related to the pit sizes. The stress concentration coefficient is the ratio of local maximum stress to the nominal stress which can describe the local stress. Tian et al. [7], Liu et al. [8], and Rebak and Perez [9] obtained the coefficient relationship between pit depth and stress concentration, assuming fixed pit width and length through physical model tests. In addition, Guo et al. [10] established a pit model by programming and obtained the relationship between stress concentration and pit length, width, and depth, respectively.

The current researches related to the effects of the aforementioned two impact factors on the fatigue life of steel strands either considered the variable only or taken into account the chloride-induced corrosion separately. So, the coupling effects of variable and chloride-induced corrosion on the fatigue of steel strands required to be further explored and discussed. This paper investigates the fatigue life of steel strands with the coupling effects of the variable and chloride-induced corrosion action. Furthermore, we explored the pit evolution law of steel strands and analyzed the corrosion mechanical mechanism; the results show that the relation of corrosion weight loss to tensile strength and elongation are subjected to the exponential function and linear relationship, respectively. Additionally, a new formula was established based on the three-dimensional linear regression theory to illustrate the relationship between the pit size and the significant concentration factor also be called SCF. Ultimately, a predicted model was proposed to investigate the fatigue life of steel strands with pits in different size. To verify the effectiveness of the theoretical by numerical modeling, models were established by the software of ANSYS. The numerical solution compared with the theoretical results seemed to be closer, indicating that they are reasonably effective in practical applications under the coupling effects. These findings are expected to be helpful in realistically predicting the durability of the cable structures.

2. Experiment

2.1. Test Specimen. The experiment box in Figure 1 is used to simulate the coupling effect of loads and environment, and the material of steel strand is composed of carbon steel and other metals (except Fe, C:0.83~0.86%, Mn:0.62~0.84%, Si: 0.12~0.20%). The length of the specimen is 10 cm, the error within 5%. The steel strands composed of seven high-strength steel wires have been widely used in practical. And the radius of them are about 15.2 mm; the tensile strength and the galvanized layer are 180 MPa and 110g/m^2, respectively.. Both ends of the steel strand are applied with alternating loads by jacks and reaction walls. The load amplitudes are $\Delta\sigma = 100$ MPa, $\Delta\sigma = 200$ MPa, and

$\Delta\sigma = 300$ MPa. The maximum load is $0.4 f_{ptk}$ (744 MPa [11], f_{ptk} is the standard value of ultimate strength of steel strand). Single loading cycle is 4 hours, and the upper and lower limits stress is converted every 2 hours. The equipment used in the test is shown in Table 1. After the test, the corrosion morphologies of the steel strand are observed by an industrial electron microscope, as shown in Figure 2. In order to analyze the distribution of corrosion pits, we measured the pit sizes under three working conditions.

To ensure the accuracy of the test, the specific chloride corrosion solution configuration is shown in Table 2 [11].

Chloride corrosion solution (5000 ML) is made of 5% NaCl, 94.37% H$_2$O, 0.03% CuCl$_2$ 2H$_2$O, and 0.60% CH$_3$COOH. When preparing the solution, put the sodium chloride into the pure water at first, the concentration is controlled at about 50g/L. After mixing copper dichloride (CuCl$_2$·2H$_2$O) with the concentration of 0.26 g/L, add glacial acetic acid to control the pH value of the salt spray solution between 3.1 and 3.3 with temperature kept at 25°C [9–11]. After the test, the corrosion products on the surface of steel strands are cleaned by distilled water and dried, and residual corrosion products on surface or gaps that cannot be wiped off mechanically need further operations. 1000 ml chromic acid solution with 200 g chromium trioxide and distilled water is prepared, and 10 g silver nitrate is added into the solution to prevent residual chloride ions from attacking the matrix of the steel strands, and then cleaned up with pure water and dryed up.

3. Analysis of Test Results

Corrosion time and stress amplitude are two important factors affecting the corrosion mechanical properties of the steel strand. In order to explore the specific influence of corrosion time, the tensile strength and elongation of the steel strand are measured after 120 h, 360 h, 600 h, and 720 h of the experiment, respectively, under fixed stress amplitude. Specific steps are as follows: the specimen is cut to about 1 m in each section and loaded with a tensile testing machine, as shown in Figure 3, and cylinder displacement is used to replace the extensometer elongation to avoid damage of extensometer clamped on steel strand by tension expansion in experiment. In the preloading stage, the speed is kept at 2 mm/min, and once the target load (2 kN) is reached, the directional tension is carried out at the speed of 1 kN/sec until fracture [12–14].

Conclusions drawn are shown in Table 3.

Table 3 shows the changes of mechanical properties of steel strands under various corrosion times. Seventy hours later, the steel wire is almost free of corrosion due to the protection of zinc coating, the corrosion weight loss is less than 10 g, and both the tensile strength and elongation are within normal range. 120 hours later, plenty of white rust and a little red rust appear on the galvanized layer of steel wire. The corrosion weight loss is between 10 g and 150 g, and the matrix of steel strands begins to corrode, leading to the slight decrease in tensile strength and elongation. 360 hours after the test, a large number of red rusts appear on the steel wire, and a few pits are also found after cleaning. The

FIGURE 1: Inner structure of salt spray corrosion test chamber.

TABLE 1: Test equipment [11].

Device name	Specification type	Technical parameter	Quantity (unit)
Salt fog test box	YC-200	Saline spray deposition, 250 ml/m^2/h	1
Universal testing machine	WAW-1000	Maximum load, 1000 kN	1
Air compressor	VB-0.2/8	Power, 2.2 kW	1
Digital scanning electronic instrument	KYKY-2008B	—	1
Electronic balance	SL500 ZN	Accuracy, 0.01 g	1
Ultrahigh-voltage electric oil pump	DSS	Power, 0.75 kW	1
Acidimeter	PHS-3C	—	1

(Table 2 is reproduced from Xuanrui et al., Numerical and Experimental Study on the Steel Strands under the Coupling Effect of a Salt Spray Environment and Cyclic Loads. Materials, 2019; 13 (3)).
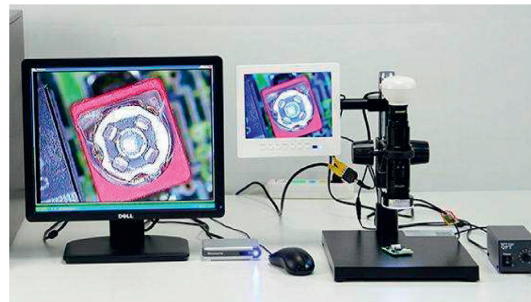
FIGURE 2: The industrial electron microscopy.

TABLE 2: Chemical composition of salt solution [11].

Chemical composition	NaCl (g)	H$_2$O (mL)	CuCl$_2$·2H$_2$O (g)	CH$_3$COOH (mL)
Content (5000 ml)	250	4718.7	1.3	30
Percent	5	94.37	0.03	0.60

(Table 2 is reproduced from Xuanrui et al., Numerical and Experimental Study on the Steel Strands under the Coupling Effect of a Salt Spray Environment and Cyclic Loads. Materials, 2019; 13 (3)).

FIGURE 3: The tensile testing machine.

TABLE 3: The corrosion parameters of steel strands.

Corrosion time (h)	Figure	Corrosion weight loss (g/m^{-2})	Tension strength (MPa)	Breaking elongation A (%)
70		≤10	1850–1890	≥5.5
120		10~150	1710–1860	5.0~5.5
360		150~300	1620–1830	4.2~5.0
600		300~400	1350~1550	3.2~4.2
720		≥400	≤1350	≤3.2

corrosion weight loss is between 150 g and 300 g, and the tensile strength and elongation begin to decrease obviously. After 600 hours, many parts of the steel wire are corroded or damaged. After cleaning the corrosion products, there are numerous dense corrosion pits. The corrosion weight loss is between 300 g and 450 g, and the tensile strength and elongation decrease obviously. Having carried out for 720 hours, most of the steel wires are severely rusted with visible corrosion cavities, which are connecting with each other to form larger pits. After cleaning the corrosion products, pits of large scales have formed. Dissolving a few corrosion products in hydrochloric acid solution, with KSCN solution, we find the solution becomes red (Fe (SCN)$_3$), indicating that plenty of Fe^{3+} exist in the corrosive products.

Steel strands are graded according to the weight loss, as shown in Table 4 [12].

The relationship between corrosion weight loss and tensile strength and elongation of steel strands is shown in Figure 4.

Figure 4(a) shows the relationship between corrosion rate and tensile strength ($R_2 = 0.95$), and Figure 4(b) indicates relationship between corrosion rate and elongation

TABLE 4: Division standards of steel strands [12].

Classification	I	II	III	IV
The pit density	0~150 g	150%~300 g	300 g~450 g	450 g~600 g

($R_2 = 0.93$), which are of great fitting degree. The relationships between corrosion rate and tensile strength and elongation of steel strand are described in the following equations, respectively:

$$\sigma_{ut} = 2047 - 195e^{4\Delta w}, \tag{1}$$

$$\varepsilon = 6 - 7\Delta w, \tag{2}$$

where σ_{ut} is the tensile strength of steel strand (MPa), ε indicates the elongation, and Δw represents the corrosion rate.

The above results show that the corrosion rate and tensile strength of steel strand obey exponential distribution and linear distribution with elongation, and after the experiment, all the pit sizes on the component surface are measured. The specimens were observed by an industrial microscope in
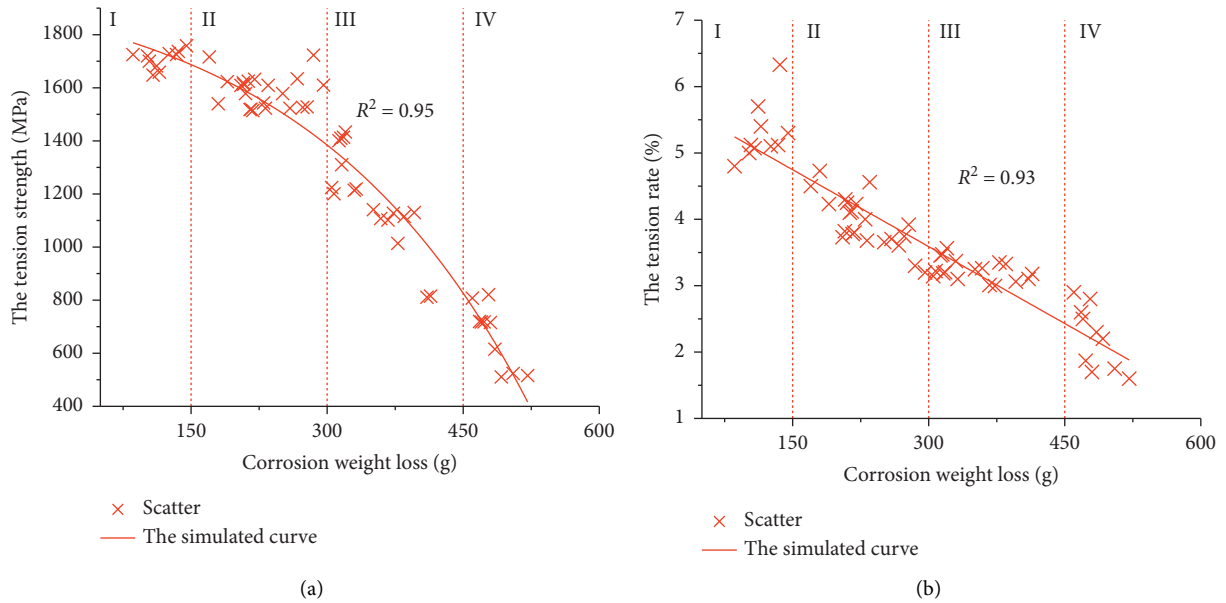
(a)

(b)

FIGURE 4: Relationship between corrosion loss and mechanical indexes.

boosting 170 times to obtain the measurement including the length and the width of the corrosion pit, as shown in Figure 5, and the depth of pits is measured by a profilometer [13]; its accuracy can reach millimeter level. The results are show in Figure 6.

4. Numerical Simulation Analysis

The numerical model is proposed by ANSYS software. Solid 95 element was used to simulate the complex analysis. A moderate length of steel strands should be chosen not only to minimize the effects of end condition but also can solve the computation time. A much longer steel strands length could require much heavier computational loads. The determination of steel strands is a tradeoff between accuracy and efficiency. The model of 10 cm in length is recommended by the literature [14]. The elastic modulus of the steel strand is (En = 2.1e11 Pa); the Poisson's ratio is 0.3. The pit size is referred to Figure 6. One end of the steel strands is fixed, and the displacement was limited in all three directions. The other end is free; the tension force is applied on the surface of it. The element type is solid 45 (high-order element solid 95 is used for the extremely irregular parts). The whole model is meshing from top to bottom by mapping grid, and the grids around pits are smaller, keeping the accuracy at 0.1 mm [15]. While the grids away from pits are larger where the maximum side length is 0.5 mm, the number of model elements and nodes are 49762 and 98347, respectively, and the pit sizes and spacing are determined according to the test results. Part of the model grid is shown in Figure 7.

The loading diagram of steel strand is shown in Figure 8. Tensile stress of 1860 MPa is applied at the free end.

Partial results are shown in Figure 9.

Figure 9 shows that the obvious stress concentration phenomenon has formed at pit position under tensile stress,
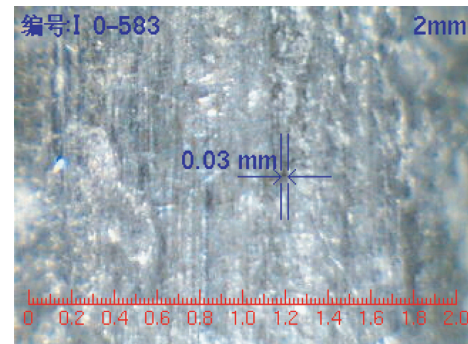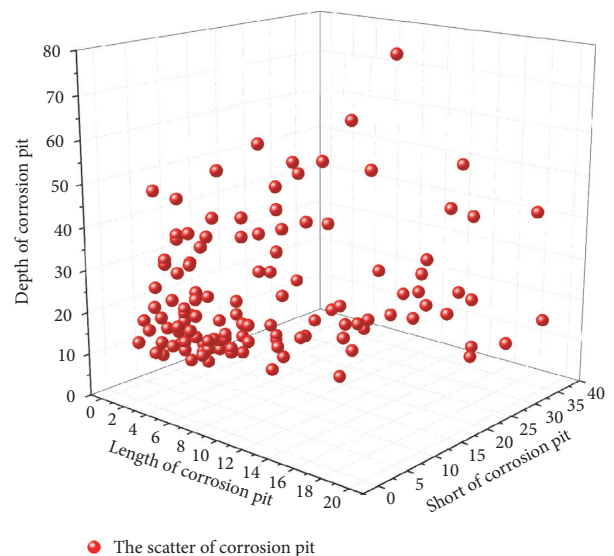

FIGURE 5: The measurement results of pit sizes.
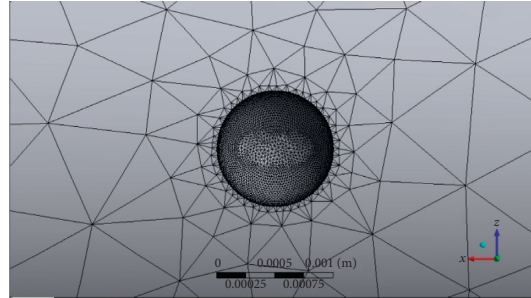

FIGURE 6: The distribution of scattered points of pits (μm).
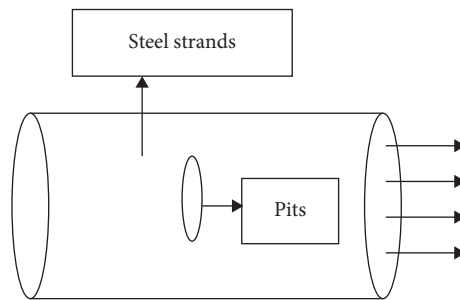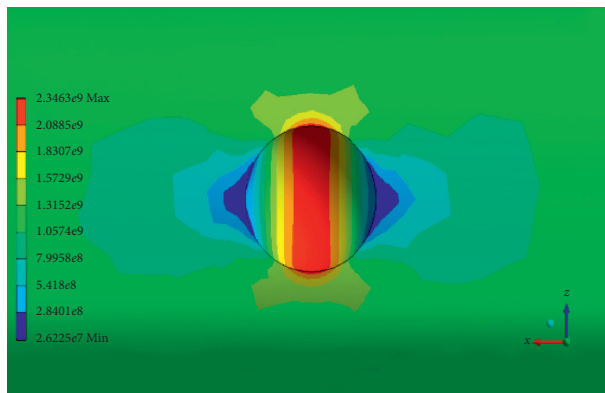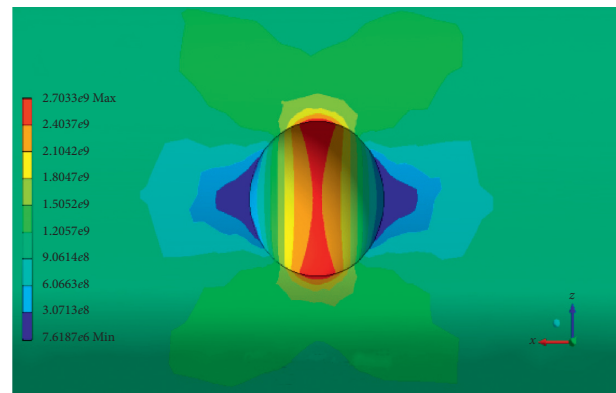
FIGURE 7: The model grid.

FIGURE 8: Schematic diagram of the model loading.

(a)

(b)

FIGURE 9: Pit stress diagram.

and with the increase of pit width, the tensile stress areas gradually shift from the bottom to both sides of pits, and the maximum stress also changes, indicating that apart from the pit depth, the length and width also have great influence on the stress distribution and maximum stress. In order to explore the influence of pit length on the maximum local stress, the relationship between pit length, width, depth, and stress concentration factor is obtained by multidimensional linear regression theory, providing a reference for evaluating corrosion fatigue life of steel strand.

The result to the fatigue life of steel strands predicted by the numerical model is shown in Figure 10.

The numerical solution shows that the fatigue life of steel strands is mainly affected by the depth of pits, and the fatigue life of steel strands is reduced with the depth of pits

increased. As shown in Figures 10(a) and 10(c), the length and the width of the model in Figure 10(a) are larger than that in Figure 10(c) and the depth of pits is proportional to the SCF, reducing the fatigue life deeply. Additionally, the length and the width both have a little effect on the fatigue life of steel strands. As shown in Figures 10(c) and 10(d), when the depth of pits is constant, the pits in different lengths and widths probably have the same SCF value.

5. Linear Regression Analysis

The main process of linear regression analysis is as follows: (1) multiple linear regression model establishment; (2) regression parameter estimation; (3) regression model test; (4) regression parameter test.
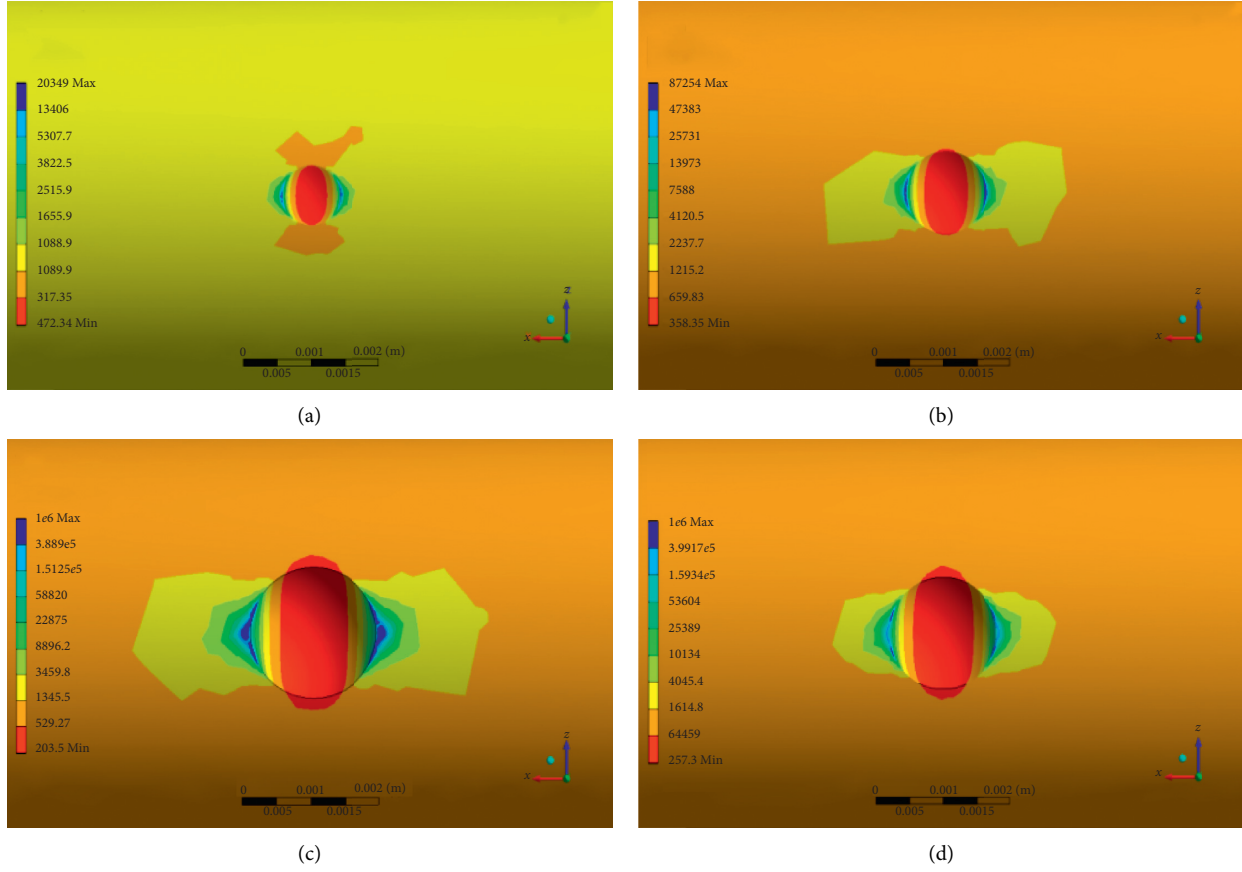
FIGURE 10: The fatigue life of steel strands with pits in different size. (a). $a_i = 0.2\,\text{mm}, b_i = 0.1\,\text{mm}, c_i = 0.4\,\text{mm}$, (b) $a_i = 0.3\,\text{mm}$, $b_i = 0.2\,\text{mm}, c_i = 0.25\,\text{mm}$, (c) $a_i = 0.4\,\text{mm}, b_i = 0.3\,\text{mm}, c_i = 0.2\,\text{mm}$, and (d) $a_i = 0.45\,\text{mm}, b_i = 0.4\,\text{mm}, c_i = 0.2\,\text{mm}$

The multiple linear regression equation is as follows [16]:

$$\text{SCF} = \beta_0 + \beta_1 a_i + \beta_2 b_i + \beta_3 c_i + \xi, \tag{3}$$

where ξ obeys the normal distribution $(0, \sigma^2)$, β_0, β_1, β_2, and β_3 are estimation parameters, a_i, b_i, and c_i stand for the pit length, width, and depth, respectively, and SCF is the stress concentration factor corresponding to the pit. SCF $= \sigma_i/\sigma_0$, where σ_i is the local maximum stress of steel strand, which can be automatically searched by software, as shown in Figure 10, and σ_0 is the nominal stress of the strand, i.e., the stress applied at both ends of the strand.

The correlation coefficient ($R_2 = 0.853$) of the regression model shows that the pit size parameter is highly linear related to the stress concentration factor, ensuring the accuracy of the model, and the parameter test is usually based on the t-value. T-test is mainly used for positive distribution with unknown population standard deviations. T-test uses the t-distribution theory to derive the probability of the difference to compare whether the difference between the two means is significant. The values of parameters and the test results of t-value are shown in Table 5.

The relationship between stress concentration factor and the length, width, and depth of pits is shown below:

TABLE 5: Parameter values of the multidimensional linear regression equation.

Regression parameter	Parameter value	Value (t)	Inspection level
β_0	1.201	−3.216	1.2e−7
β_1	15.42	10.178	1.3e−8
β_2	−6.86	−4.532	1.5e−7
β_3	8.47	3.112	4.1e−8

$$\text{SCF} = 1.201 + 15.42a_i - 6.86b_i + 8.47c_i. \tag{4}$$

Equation (4) shows that the pit length, width, and depth are directly proportional to the stress concentration factor, and greater width will lead to lower local maximum stress (a_i ranges from 0 to 0.02 mm, b_i ranges from 0 to 0.04 mm, and c_i ranges from 0 to 0.08 mm, as shown in Figure 5).

6. Model to Predict the Fatigue Life of Steel Strands

Pit sizes have great impact on local stress concentration on the surface of the steel strand; with increasing local stress, the derivation of crack may lead to the damage of the steel
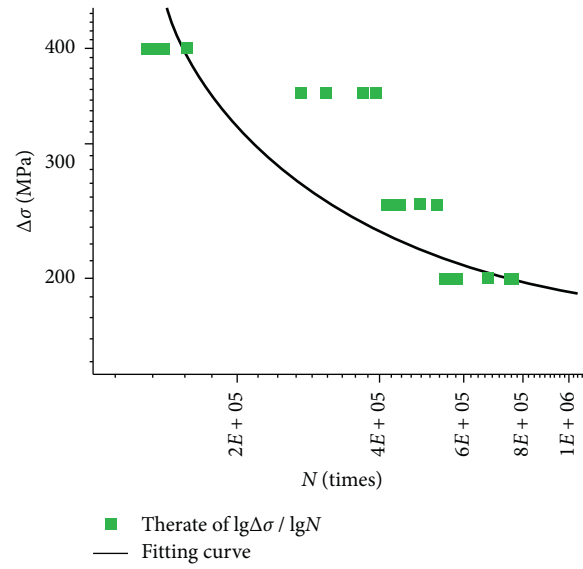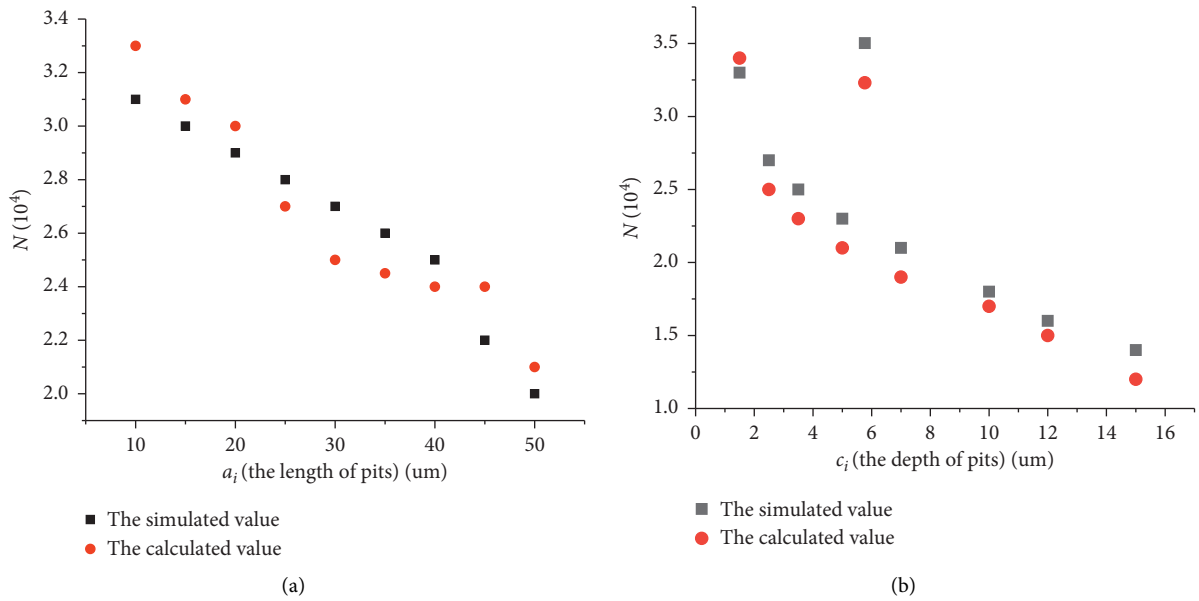
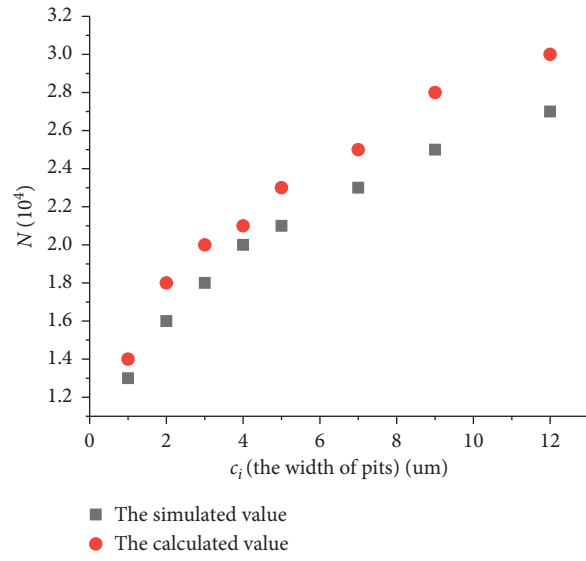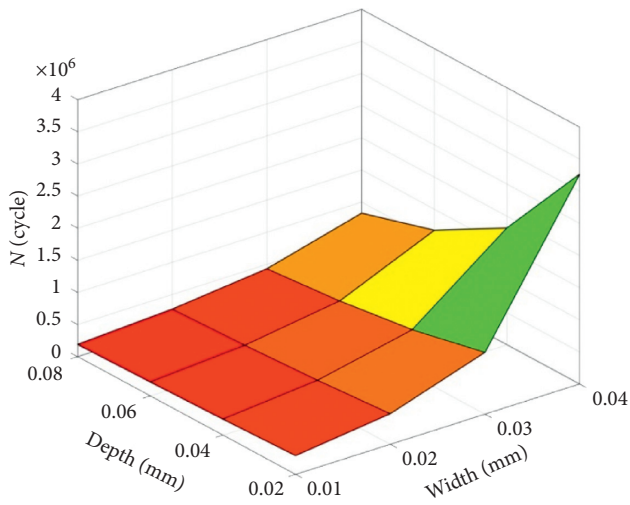FIGURE 11: Corrosion fatigue life of steel strand.
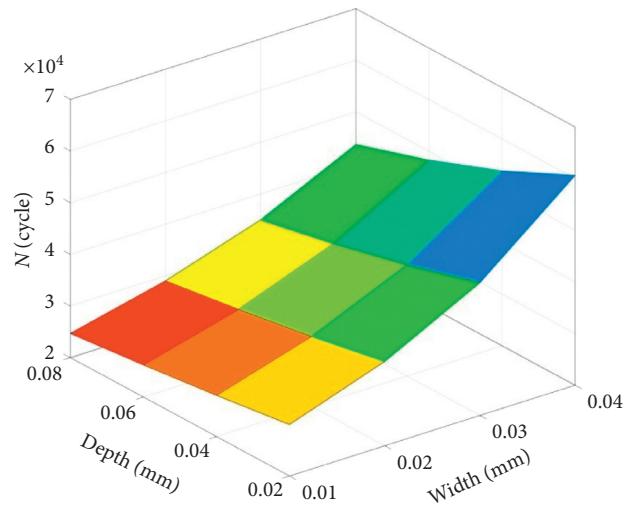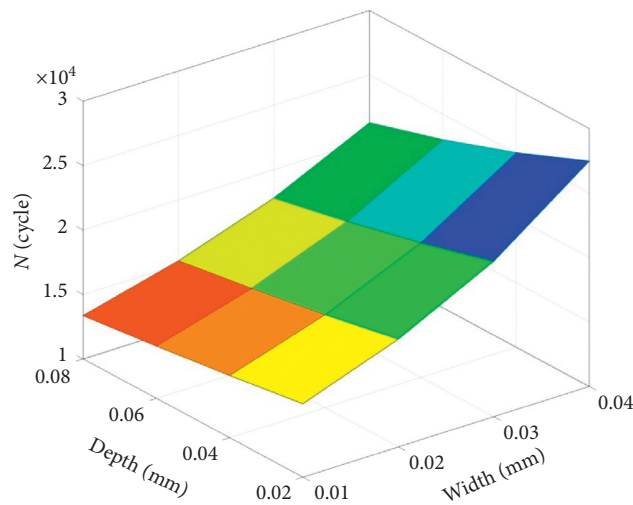

(a)

(b)

FIGURE 12: Continued.

(c)

FIGURE 12: The comparison results between numerical solution and theoretical solution.

(a)

(b)

(c)

FIGURE 13: When a_i = 0.01 mm, the relationship between pit size and corrosion fatigue life of steel strand. (a) $\Delta\sigma$ = 100 MPa, (b) $\Delta\sigma$ = 200 MPa, and (c) $\Delta\sigma$ = 300 MPa.

(a)

(b)

(c)

FIGURE 14: When $a_i = 0.02$ mm, the relationship between pit size and corrosion fatigue life of steel strand. (a) $\Delta\sigma = 100$ MPa, (b) $\Delta\sigma = 200$ MPa, and (c) $\Delta\sigma = 300$ MPa.
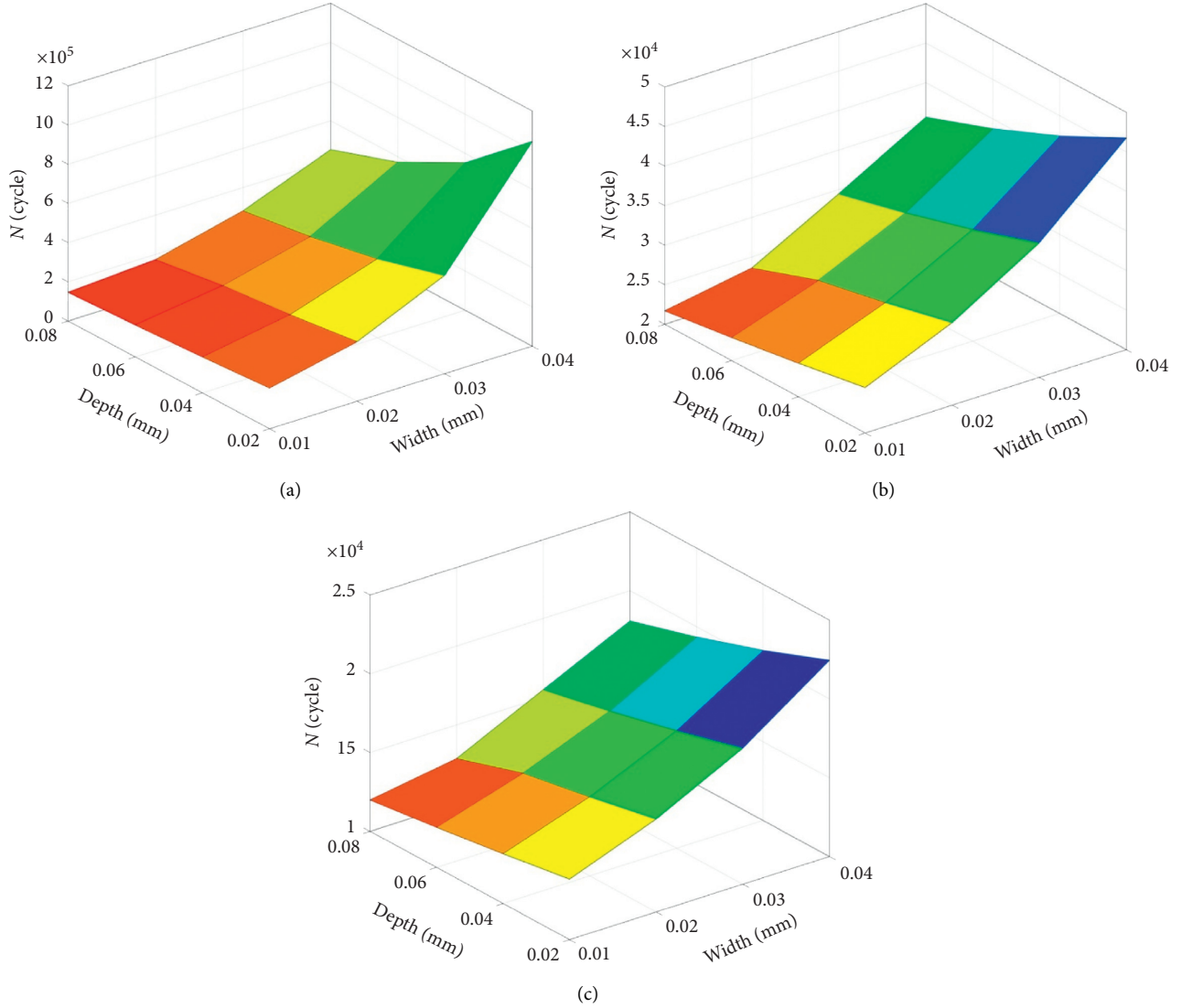
strand. Therefore, it is quite important to explore the relationship between the pit size and the fatigue life of the steel strand, which can provide a reference for further prediction of the fatigue life of the cable. A perfect expression of fatigue crack initiation life has been proposed by Zheng et al. [17, 18] to analyze the fatigue characteristics of metal materials in different states, as shown in the following equation:

$$N = C_i \left(\Delta\sigma_{eqv}^{2/1+n} - \left(\Delta\sigma_{eqv} \right)_{th}^{2/1+n} \right)^{-2}, \qquad (5)$$

$$\Delta\sigma_{eqv} = \sqrt{\frac{1}{2(1-R)} F_i \Delta\sigma}, \qquad (6)$$

where C_i stands for the initial crack resistance coefficient of the material, R represents the stress ratio, F_i is the stress concentration coefficient, $\Delta\sigma$ is the stress amplitude, and N is the strain strengthening coefficient. Arola and Williams [18] puts forward that in the condition of torsion, the strain

strengthening coefficient $n = 1$, and in the case of stretching, the strain hardening coefficient $n = 2$. $(\Delta\sigma_{eqv})_{th}$ is the cracking stress value of the material, which is related to the tensile property, when $\Delta\sigma_{eqv} \leq (\Delta\sigma_{eqv})_{th}$, $N \longrightarrow +\infty$, which means that steel strands will not be damaged by load. $(\Delta\sigma_{eqv})_{th}$ and C_i are determined by experiment, as shown in Figure 11.

The value of C_i is about 10^7, and the value of $(\Delta\sigma_{eqv})_{th}$ is about 185 MPa. Equation (5) can be expressed as follows:

$$N = 10^7 \left(\Delta\sigma_{eqv}^{2/3} - (185)^{2/3} \right)^{-2}. \qquad (7)$$

From the above analysis, a new formula was proposed to investigate the fatigue life of steel strands with pit in different size. The result shows that the width is proportional to the fatigue life of steel strands but for the length and the depth of the pits to the fatigue life of steel strands have an opposite effect. To verify the effectiveness of theoretical solution by numerical modeling, the models established by ANYSIS in

different pit size are compared with the theoretical solution. The partial comparison result is shown in Figure 12.

The width is proportional to the fatigue life of steel strands but the length and the depth have the opposite effects on that. The numerical solution is closer to the theoretical solution; the relative error is within 10% range, indicating that the theoretical solution is reliability.

At present, the corresponding code illustrating the fatigue life of steel strands with pits is not available. Therefore, the relative base data should be built to investigate the fatigue life of steel strands with pits in different size. The prediction fatigue life of steel strands with pits in different size was calculated by equation (7) for three different stress amplitudes; the results are shown in Figures 13 and 14.

Figures 13 and 14 show the fatigue life of steel strands with pits in different sizes and under different stress amplitudes 100 MPa, 200 MPa, and 300 MPa (when the length of pit is $a_i = 0.01$ mm and $a_i = 0.02$ mm, respectively). The pictures indicate that the corrosion fatigue of steel strand is mainly determined by pit size and the magnitude of alternating load. When the pit length is constant, the corrosion fatigue life of the steel strand will further decrease with the increase of pit depth, but the reduction rate will decrease with the expansion of pit width, indicating that the increase of pit width can delay the cracking rate of the steel strand, and the corrosion fatigue life curve of the steel strand obtained is conductive to further evaluating the reliability of cable supported bridges.

7. Conclusion

In this paper, the corrosion process of the steel strand is simulated by salt spray corrosion test; the corrosion pattern of the steel strand is analyzed by proposing the gray scale theory. Conclusions are that the corrosion life of the steel strand is influenced by the pit size and the stress amplitude. Besides, with numerical simulation, the relationships between the length, width, and depth of the corrosion pit and the stress concentration coefficient are obtained based on the three-dimensional linear regression method to predict the corrosion fatigue life of the steel strand. The specific conclusions are as follows:

(1) The tensile strength and elongation of the steel strand will decrease obviously with deeper corrosion, and the results of gray scale treatment show that greater stress amplitude will lead to more serious corrosion.

(2) The relationships between the stress concentration factor and pit length, width, and depth are obtained. With the method of three-dimensional linear regression, the regression equation shows that the length and depth of the pit are in direct proportion to the stress concentration factor, while the width is in inverse proportion to the stress concentration factor.

(3) The relationships between the width, length, and depth of corrosion pit and the corrosion fatigue life of steel strand are obtained, providing a reference for further analysis of the corrosion fatigue life of cables.

Data Availability

The table and figure data used to support the findings of this study are available from the corresponding author upon request.

Conflicts of Interest

The authors declare that there are no conflicts of interest regarding the publication of this paper.

Authors' Contributions

Conceptualization and software X.Y; formal analysis, G.Y.; and writing-original draft preparation, X.Y.

Acknowledgments

References

[1] K. Suzumura and S.-i. Nakamura, "Environmental factors affecting corrosion of galvanized steel wires," *Journal of Materials in Civil Engineering*, vol. 16, no. 1, pp. 1–7, 2004.

[2] I. Verpoest, E. Aernoudt, A. Deruyttere, and M. De Bondt, "The fatigue threshold, surface condition and fatigue limit of steel wire," *International Journal of Fatigue*, vol. 7, no. 4, pp. 199–241, 1985.

[3] I. Verpoest, *The fatigue threshold, the surface condition and the fatigue limit of steel wire*, PhD Thesis, K. U. Leuven, (Belgium, Germany), 1981.

[4] K. Lambrighs, M. Wevers, B. Verlinden, and I. Verpoest, "A fracture mechanics approach to fatigue of heavily drawn steel wires," *Procedia Engineering*, vol. 10, pp. 3259–3266, 2011.

[5] S. Beretta and S. Matteazzi, "Short crack propagation in eutectoid steel wires," *International Journal of Fatigue*, vol. 18, no. 7, pp. 451–456, 1996.

[6] A. Valor, F. Caleyo, L. Alfonso et al., "Stochastic modeling of pitting corrosion: a new model for initiation and growth of multiple corrosion pits," *Corrosion Science*, vol. 49, no. 2, pp. 570–579, 2007.

[7] W. Tian, S. Li, B. Wang, J. Liu, and M. Yu, "Pitting corrosion of naturally aged AA 7075 aluminum alloys with bimodal grain size," *Corrosion Science*, vol. 113, pp. 1–16, 2016.

[8] Y. Liu, A. Laurino, T. Hashimoto et al., "Corrosion behaviour of mechanically polished AA7075-T6 aluminium alloy," *Surface and Interface Analysis*, vol. 42, no. 4, pp. 185–188, 2010.

[9] P. B. Rebak and T. E. Perez, "Effect of carbon dioxide and hydrogen sulfide on the localized corrosion of carbon steels

and corrosion resistant alloys," *NACE*, vol. 89, no. 33, pp. 195–202, 2017.

[10] D. Guo, D. Guo, K. Ren et al., "Three dimensional cellular automata model of metal local corrosion," *Mechanics and Practice*, vol. 36, no. 4, pp. 173–181, 2014, (in Chinese).

[11] X. Yu, G. Yao, L. Gu, and W. Fan, "Numerical and experimental study on the steel strands under the coupling effect of a salt spray environment and cyclic loads," *Materials*, vol. 13, no. 3, p. 736, 2020.

[12] ASTIM G85–94, *Standard Practice for Modified Salt Spray (Fog) Testing*, International Helping Our World Work Better, West Conshohocken, PA, USA, 2011.

[13] A. B. M. Abdullah, J. A. Rice, H. R. Hamilton et al., "Experimental and numerical evaluation of unbonded post-tensioning tendons subjected to wire breaks," *Journal of Bridge Engineering*, vol. 21, no. 10, Article ID 04016066, 2016.

[14] M. Raoof and I. Kraincanic, "Determination of wire recovery length in steel cables and its practical applications," *Computers & Structures*, vol. 68, no. 5, pp. 445–459, 1998.

[15] Y. Xu, H. Li, S. Li, X. Guan, and C. Lan, "3-D modelling and statistical properties of surface pits of corroded wire based on image processing technique," *Corrosion Science*, vol. 111, no. 38, pp. 275–287, 2016.

[16] J. D. Herman, "Three-dimensional modeling in linear regression," *Prediction Variables*, vol. 33, pp. 234–243, 2000.

[17] Z. Xiulin, "A further study on fatigue crack initiation life - mechanical model for fatigue crack initiation," *International Journal of Fatigue*, vol. 8, no. 1, pp. 17–21, 1986.

[18] D. Arola and C. Williams, "Estimating the fatigue stress concentration factor of machined surfaces," *International Journal of Fatigue*, vol. 24, no. 9, pp. 923–930, 2002.